JPET#254540

Title: **Synergistic effects of Acetyl-L-carnitine and adipose-derived stromal cells to improving regenerative capacity of acellular nerve allograft in sciatic nerve defect**

Contributors

Ghayour Mohammad-Bagher, Department of Biology, Faculty of Science, Ferdowsi University of Mashhad, Mashhad, Iran

Abdolmaleki Arash, 1- Department of Engineering Sciences, Faculty of Advanced Technologies, University of MohagheghArdabili, Namin, Iran. 2- Bio Science and Biotechnology Research center (BBRC), Sabalan University of Advanced Technologies (SUAT), Namin, Iran.

Behnam-Rassouli Morteza, Department of Biology, Faculty of Science, Ferdowsi University of Mashhad, Mashhad, Iran

Mahdavi-Shahri Naser, Department of Biology, Faculty of Science, Ferdowsi University of Mashhad, Mashhad, Iran

Moghimi Ali, Department of Biology, Faculty of Science, Ferdowsi University of Mashhad, Mashhad, Iran

JPET#254540

Running title: Effect of Acetyl-L-carnitine on functional recovery

Corresponding Author: Name: Morteza Behnam-Rassouli, Department of Biology, Ferdowsi University, Azadi Square, Mashhad, Iran. Zip code: 9177948974 , Phone numbers: +9838805503, E-mail address: ari_1364@yahoo.com

Number of text pages: 26

Number of tables: 2

Number of Figures: 12

Number of references:47

Number of words in the Abstract: 231

Number of words in Introduction: 687

Number of words in Discussion:1500

Section : Neuropharmacology

JPET Fast Forward. Published on December 27, 2018 as DOI: 10.1124/jpet.118.254540
This article has not been copyedited and formatted. The final version may differ from this version.

Abstract:

Purpose: The combination of decellularized nerve allograft and adipose-derived stromal cell (ASCs) represents a good alternative to nerve autograft for bridging peripheral nerve defects by providing physical guiding and biological cues. However, regeneration outcome of acellular nerve allograft (ANA) is often inferior to autograft. Therefore, we hypothesized that Acetyl-l-carnitine (ALCAR) treatment and implantation of ASCs embedded ANA would work synergistically to promote nerve regeneration. **Methods:** Seventy rats were randomly allocated into seven experimental groups (n = 10) including the healthy control group, sham surgery group, autograft group, ANA group, ANA + ASCs group, ANA + ALCAR group (50 mg/kg for two weeks) and ANA + ASCs + ALCAR (50 mg/kg for two weeks) group. All grafts were implanted to bridge long-gap (10 mm) sciatic nerve defects. Functional, electrophysiological and morphological analysis was conducted during the experimental period. **Results:** We found that the ALCAR potentiated the transplanted survival and retention of ASCs and upregulates the expression of neurotrophic factors mRNA in transplanted graft. Sixteen weeks following implantation in the rat, the ANA supplemented by ASCs is capable of supporting the re-innervation across a 10 mm sciatic nerve gap, with results close to that of the autografts in terms of functional, electrophysiological and histological assessments. **Conclusions:** Results demonstrated that ALCAR treatment improved regenerative effects of ANA combined with ASCs on reconstruction 10 mm sciatic nerve defects in rats as comparable to those of autograft.

Introduction

Peripheral nerve injury (PNI) is a common disorder in the clinic. Direct nerve coaptation is the preferred method for repair of nerve transection in the absence of nerve gap. But, in the cases that direct repair is impossible, the current clinical gold standard treatment is the nerve autograft (Siemionow, Bozkurt, & Zor, 2010). However, clinical application of autograft is limited by the availability of donor nerves, donor site morbidity and a size mismatch between the donor nerve and the recipient nerve (Mackinnon & Hudson, 1992; Neubauer, Graham, & Muir, 2010). This has led to the development of alternatives to autologous nerve grafts. In this regard, the combination of decellularized nerve allograft and stem cells represents a good alternative to nerve autograft that could be used in the clinic. Acellular nerve allograft preserve the nerves internal structure that facilitates axonal regeneration. Furthermore, decellularization processes prevent immunological rejection by removal of antigenic cellular components. However, regeneration outcome of acellular nerve allograft is often inferior to autograft, perhaps due to lack of cellular component specially Schwann cells. Schwann cells are an essential component for peripheral nerve regeneration. They are involved in releasing growth factors and re-myelination regenerated axons (Jessen & Mirsky, 2008). It seems that employment of acellular allograft nerve seeded with Schwann cells is an effective method to repair peripheral nerve defects (Doolabh, Hertl, & Mackinnon, 1996). However, the difficulties in the harvesting and expansion of Schwann cells beside the morbidity of the donor's site strongly limit their use in regenerative medicine (Kingham et al., 2007; Tohill & Terenghi, 2004). Therefore, Schwann-cell like cells derived from stem cells are an attractive alternative because they can be obtained from the patient for use in an autologous therapy (Brohlin et al., 2009). Autologous cells are generally considered to be more readily accepted by the patient because they do not provoke an immune reaction (Mosahebi, Fuller, Wiberg, & Terenghi, 2002). In this regard, adipose-derived stem cells (ASCs) are an easily accessible source of adult stem cells that have interested as candidates for autologous cell

transplantation. (di Summa et al., 2011; Kuroda et al., 2010; McKenzie, Gan, Doedens, Wang, & Dick, 2006). The adipose tissue is a mesodermally derived complex tissue that besides adipocytes, contains a stromal population which includes non-adipocyte cells such as stem cells (Kokai, Rubin, & Marra, 2005). According to the nomenclature established by the International Fat Applied Technology Society, ASCs are adipose-derived MSCs that are adherent in plastic culture dishes (Gimble, Katz, & Bunnell, 2007). ASCs ability to differentiate into the glial cell line make them a excellent candidates for use as an alternative to Schwann cells for peripheral nerve repair (Kingham et al., 2007; Locke, Windsor, & Dunbar, 2009). These properties of ASCs, making them attractive cell sources for tissue engineering and regenerative medicine (Gimble et al., 2007). However, the low survival rate and retention of transplanted ASCs limits their therapeutic potential (Potier et al., 2007). It has been shown that most of the transplanted ASCs are lost due to the harmful microenvironment of injured tissues, such as oxidative stress, energy failure, growth factor deprivation, inflammatory response and subsequent apoptosis (Toma, Pittenger, Cahill, Byrne, & Kessler, 2002). Therefore, any approach that enhances survival and retention capacity of ASCs may improve the nerve regeneration process and consequence functional recovery. In this regard, Acetyl-l-carnitine (ALCAR, $C_9H_{17}NO_4$) is an acetylated carnitine [3-hydroxy-4-(trimethylammonio)butanoate] derivative with anti-apoptotic and antioxidant properties (Mansour, 2006; Tesco et al., 1992). Also, it shows protective effects on the traumatic neural injuries (Fernandez et al., 1989; Hart, Wiberg, Youle, & Terenghi, 2002). ALCAR interacts with the mitochondrial membrane and plays an important role in the mitochondrial oxidation of fatty acids and production of cellular energy (Lu, Zhang, & Elisseeff, 2015). It seems that ALCAR reduced cytosolic levels of cytochrome-C and subsequent caspase-3 activation (Di Cesare Mannelli et al., 2007). We hypothesized that ALCAR treatment and transplantation of ASCs into decllularized nerve allograft would work synergistically to promote nerve regeneration. Therefore, this experimental study was conducted to evaluate the effect of co application of systemic

administration of ALCAR and ASCs supplemented nerve allograft on bridging a 10-mm gap in the sciatic nerve.

Materials and methods:

Animals

All experimental procedures were conducted in accordance with the European Communities Council Directive of 24 November 1986 and the guidelines of the Ethics Committee of the Ferdowsi University of Mashhad (Iran). All experiments were performed on adult male Wistar rats (200–250 g). Animals were housed under standard laboratory conditions (temperature, 22±2 °C, 12-h light/dark cycle and 60 ± 5% humidity) with free access to food and tap water *ad libitum*.

Experimental groups

Seventy rats were randomly allocated into seven groups (n = 10), including healthy control, sham surgery, acellular nerve allograft (ANA) without any treatment, ANA seeded with ASCs, ANA treated with ALCAR, ALCAR treatment ASCs–ANA construct and autograft as a positive control group. Two experimental groups were treated daily with ALCAR at the doses of 50 mg/kg for two weeks. ALCAR treatment started immediately after surgery. Regeneration through the ANA that treated with ALCAR was compared to regeneration in untreated ANA and autografts. The results of the sham group were similar to the control group therefor in order to avoid giving ineffective information the results of sham group were not presented.

Isolation, culture and identification of ASCs

ASCs were harvested from the inguinal fat pad of adult male Wistar rats as previously described (Kingham et al., 2007). In brief, the adipose tissue was enzymatically digested using 0.15% (w/v) type I collagenase (Invitrogen, UK) for 1 h at 37 ºC. Then, enzyme activity was neutralized by adding Phosphate Buffered Saline (PBS) supplemented with 1% (v/v) fetal bovine serum (FBS).

JPET Fast Forward. Published on December 27, 2018 as DOI: 10.1124/jpet.118.254540
This article has not been copyedited and formatted. The final version may differ from this version.

The stromal-vascular fraction (SVF) was then collected by centrifugation at 800 g for 5 min. Then, SVF was re-suspended in low glucose DMEM containing 10% (v/v) FBS and 100 U/ml penicillin/100 μg/ml streptomycin (Gibco) and the cells were cultured in 75 cm^2 flasks (SPL) at a density of $1 \times 10^4/cm^2$. The cultures were maintained at 37°C with 5% CO_2. Cells of passages 3-4 were used in our experiments. To confirm multipotency, ASCs at passage 3 were cultured in adipogenesis and osteogenesis differentiation media (Invitrogen, USA) according to manufacturer's protocol. Culture was changed every 3 days. After 3 weeks of culture, ASCs were subjected to Oil Red O staining for adipogenesis. Also, osteogenesis were stained with Alizarin Red for matrix mineralization. To confirm ASCs phenotype, 1×10^5 cells/ml cultured cells at passage 3 were subjected to flow cytometry for determining the surface expression of CD11b, CD29, CD31, CD45 and CD90 markers (BD Biosciences, USA), as described by the manufacturer. Cells stained with FITC-conjugated IgG1κ, IgA and IgM were used as isotype controls. Flow cytometry was performed by BD FACSCalibur flow cytometer (BD Biosciences) and analysis was performed using FlowJo v 10 (TreeStar) software.

ANA preparation

Sciatic nerves from male Wistar rats were decellularized as previously described by Sondell (Sondell, Lundborg, & Kanje, 1998). In brief, bilateral sciatic nerves were harvested and trimmed to 15 mm under aseptic conditions. Then, the nerve tissues were agitated in deionized distilled water for 7 hours. The nerve tissues were then exposed to 3 % Triton X-100 (Sigma) in distilled water for 12h, followed by a 24 h agitation in a solution of 4 % sodium deoxycholate (Sigma) in distilled water. These steps were repeated again and after a final wash with distilled water, acellular nerve segments were stored in PBS (pH 7.4) containing 100 μg/mL penicillin and 100 μg/mL streptomycin at 4°C until use. The ends of the tissue were trimmed immediately prior to implantation to attain a clean-cut, 10 mm graft. H&E staining and scanning electron microscopy (SEM) were used to observe the histology and ultrastructure of the ANA, respectively.

Histological evaluation of ANA

ANA and intact nerve segment were stained with a Harris Hematoxylin and Eosin (H&E) for observation of general morphology. Briefly, the tissue samples that fixed in 10 % formalin were paraffin-embedded, and transverse sections of 5 µm were prepared with a microtome. Tissue sections were deparaffinized by xylene and rehydrated with graded alcohols to 50% ethanol. After stained with harris hematoxylin and eosin according to standard procedures, the samples dehydrated with graded alcohols, cleared in xylene, and mounted in balsam. After drying, the sections mounted in Canada balsam under a coverslip and the slides were observed under a light microscopy (Olympus, Japan). Also, to confirm myelin and axon elimination, transverse sections of ANA stained with toluidine blue as described previously (Raimondo et al., 2009). Briefly, tissue samples were fixed in 4% paraformaldehyde and dehydration with ascending ethanol passages. The specimens were embedded in resin and serial cross-sections for each sample were cut at 1µm thickness with an ultramicrotome. For tissue analysis, resin sections were stained with 1% toluidine blue (Fluka) and the prepared slides were observed under a light microscopy (Olympus, Japan).

DAPI staining

To confirm cells elimination, transverse sections of ANA stained with DAPI as described previously. Briefly, tissue sections were deparaffinized by xylene and rehydrated with graded ethanol. The slides were drained and incubated with DAPI staining solution (200 µl) for 15 min in dark. The slides were mounted with Entellan and observed under fluorescence microscope.

Tensile Testing of ANA

ANA were loaded onto a Universal Testing Machine (SANTAM-STM20, Tehran, Iran). Specimens were attached to the tensile tester. Each specimen was stretched at a constant rate of 0.05 mm/s to complete tensile failure. The mean specimen length (n = 10/group) was 10 mm and

samples were kept moist by applying PBS to the specimen. Normal sciatic nerves were used as controls.

In vitro biocompatibility assay of ANA

Briefly, 1×10^6 ASCs were seeded onto each of the prepared ANA (5 mm) under a stereo microscope (Nikon, Japan). The cells–ANA combinations allowed attaching at 37°C for 4 h. Then, cells–ANA combinations were placed in six-well plates containing Dulbecco Modified Eagle Medium (DMEM) with 10 % fetal bovine serum for 24 h at 37 ºC and 5% CO2 under saturated humidity. After the constructs were cultured for 24 h, cell attachment was evaluated by SEM micrographs. To evaluation of ANA biocompatibility, the viability and proliferation of ASCs that seeded on ANA was compared with ASCs were cultured in 96 well plates. Briefly, 10 µL ASCs suspension with a density of 3×10^5/ml was seeded onto the 5 mm ANA and allowed attachment for 4 h. Then, cells–ANA combinations incubated on 96-well plate containing (DMEM) with 10 % FBS at 37ºC with 5% CO_2 for 96 h. In the control group, ASCs were cultured in 96 well plates at a same density. MTT assay was performed every 24 h. Briefly, samples were incubated with 20 µl MTT reagent (5mg/ml) in the dark at 37 °C for 4 h. After the addition of 200 µl dimethyl sulfoxide (DMSO; Sigma) for 1 h, the absorbance of colored formazan products was measured at a wavelength of 570 nm by a microplate reader (model 550; Bio-Rad Laboratories, Hercules, CA, USA). Absorbance values correspond to the number of viable cells. Tissue culture polystyrene (TPS) and untreated ANA were used as controls.

Surgical procedure and implantation

Before implantation, 1×10^6 ASCs were resuspended in 20µl of DMEM and injected into the ANA (10 mm). Cells-ANA combination incubated for 4 h at 37 °C with 5% CO_2 to allow cells attached to the ANA. ASCs-ANA constructs were pretreated with actyl l carnitine (10 mmol) for 12 h until surgical implantation. All experiments were performed under an operating microscope (Zeiss, Germany) under sterile conditions by the same investigator. All animals were deeply

anesthetized using an intraperitoneal injection of ketamine (80 mg/kg) and xylazine (10 mg/kg) (Alfasan Pharmaceutical Co. Holland). Animals were fixed in the prone position and the left sciatic nerve was exposed through a longitudinal incision extending from the greater trochanter to the mid-thigh. Then, the nerve was transected and a 6 mm-long segment of the sciatic nerve was removed at 1 cm below the sciatic notch. Then, a 10 mm prepared ANA was grafted to the nerve defect and fixed with four epineurial microsuture (10-0 nylon, Ethicon). For autograft, the 10 mm of the sciatic nerve was transected, reversed 180°, and then re-implanted into the nerve gap. Finally, the muscle and facia were sutured with absorbable sutures (4-0 vicryl, Ethicon) and the skin by a continuous running suture (4-0 prolene, Ethicon). The sham-operated group was subjected to the surgical procedure without the nerve defect. During the study, animals were examined for signs of autotomy and contracture. Immediately after surgery, animals in ALCAR treatment groups were intraperitoneally injected with ALCAR (sigma, italy) (50 mg/kg/day) for 14 days.

Functional assessment

The recovery of motor function was assessed by calculating the sciatic functional index (SFI) before nerve transection and at 4, 8, 12 and 16 weeks postoperative, as previously described (Dijkstra, Meek, Robinson, & Gramsbergen, 2000). The SFI value was calculated by putting the obtained data in the formula: SFI = -38.3[(EPL-NPL)/NPL] + 109.5[(ETS-NTS)/NTS] + 13.3 [(EIT-NIT)/NIT] - 8.8, where EPL: the experimental paw length, NPL: the normal paw length, ETS: the experimental toe spread, NTS: the normal toe spread, EIT: the experimental intermediary toe spread and, NIT: the normal intermediary toe spread. The SFI value varies from 0 to -100, with 0 corresponding to the normal function and -100 indicating total impairment. When no footprints were measurable, the index score of −100 was given. Sensory recovery was evaluated in the same sessions as the hot-plate test. The hot-plate is the widely used test to assess thermal nociception. In brief, the rat was wrapped in a surgical towel above its waist and then positioned to stand with the affected hind paw on a hot plate at 54°C to assess the nociceptive withdrawal reflex (WRL). WRL

is defined as the time elapsed from the onset of hotplate contact to withdrawal of the hind paw (Hargreaves, Dubner, Brown, Flores, & Joris, 1988). The cut off time for heat stimulation was set at 12 s, to avoid skin damage to the foot.

Electrophysiological evaluation

To assess the regeneration process, electrophysiological recordings were conducted at the 8 and 16 week postoperatively. For this purpose, the CMAPs peak amplitude and conduction velocity of regenerated nerves were measured between the injured side and the contralateral uninjured side as previously described (Navarro & Udina, 2009; Oğğuzhanoğğlu, Erdoğğan, Tabak, & Cenikli, 2010). In brief, the sciatic nerve was stimulated by miniature bipolar electrode, which was placed on the nerve proximal to the graft. The active and reference monopolar needle recording electrodes were inserted into the mid-belly and tendon surface of gastrocnemius muscle, respectively. A ground electrode was placed in the surrounding tissue. Stimulations (1Hz; 1 mA) with durations of 0.02 ms were given at gradually increasing intensity until a maximal CMAP response was obtained. For evaluation of motor nerve conduction (MNCV), two different points along the proximal nerve segment was stimulated. MNCVs across the segment were determined by calculations the distance between the different stimulating points and the difference in latencies (Δt). Normal nerve CMAPs and MNCV were measured from the contralateral uninjured side in a similar fashion.

Histomorphometry analysis

Following the electrophysiology study, all of the implanted grafts were harvested and subjected to toluidine blue staining for morphometric analysis as described previously. Briefly, transverse semi-thin sections (1 μm) were stained with 1% toluidine blue. Axon counts, axon diameter, and myelin thickness were calculated using the Image J program. The contralateral sciatic nerves were used as controls.

Wet gastrocnemius muscle weights

Muscle weight was measured to assess denervation atrophy at 16 weeks postoperative as previously described (Ghayour, Abdolmaleki, & Behnam-Rassouli, 2016). The gastrocnemius muscles were harvested and the mass ratio of the operated side muscle to the contralateral side muscle was calculated immediately. The muscle mass ratio represented the recovery in denervation atrophy of the gastrocnemius muscle on the operated side, with approximately 100% gastrocnemius muscle index (GMI) indicating full recovery of the operated side.

Quantitative real-time PCR

The pattern of gene expression for key markers of the Schwann cell lineage (S100 and p75) and neurotrophins (NGF, BDNF, GDNF) were compared in ASCs seeded on ANA. Also the expression of glyceraldehyde 3-phosphate dehydrogenase (GAPDH) as an internal control was evaluated. Total mRNA was extracted from tissue samples using TRIzol reagent (Invitrogen). DNase I (Fermentase, Lithuania) was used to remove DNA contamination and mRNA was quantified by spectrophotometer (Nano Drop ND-1000, Thermo Fisher Scientific). Then total RNA (5 µg of mRNA) was reverse transcribed with M-MLV (Moloney murine leukemia virus) reverse transcriptase kit (Invitrogen) [PrimeScript RT Reagent Kit (takara Bio, Dalian, China)] for cDNA synthesis. The cDNA (200 ng) was amplified in presence of 2µl Power SYBR Green Master Mix (Applied Biosystems, Foster City, CA) and 250 nM of appropriate primers using the Real-Time PCR system (Applied Biosystems; 40 cycles) and analyzed with the StepOne Software (Applied Biosystems/Life Technologies). Analyses were carried out using the ΔCt method and calculated relative to GAPDH. The results were normalized with respect to the control condition, which presented a value of 1. The following primers were used, taken from the PrimerBank webpage. The assay was repeated 3 times.

Statistical analysis

Data were analyzed with SPSS Statistics 16.0 software (SPSS Inc., Chicago, Illinois, USA). Statistical analysis was carried out using a one-way analysis of variance (ANOVA) to determine the significant differences among seven groups. Intergroup comparison of means was performed using a Tukey-*Post hoc* analysis. All data are expressed as mean ± standard error of the mean (SEM) and values of $P < 0.05$ were considered statistically significant.

Results

ASCs characterization

Under inverted phase microscopy, cultured ASCs at passages 3 had a spindle-like morphology (Fig. 1B). To confirm ASCs characterization, immunophenotype of cultured ASCs at passage 3 was performed by FACS analysis of surface marker expression. Results showed that ASCs expressed high level of CD29 (98.7±1.3%) and CD90 (98.6±0.67%), but were negative for endothelial marker CD31 (0.45±0.01%) or the hematopoietic lineage markers CD45 (2.26±0.3%) and CD11b (1.68±0.4%) (Fig. 1A). These results were in agreement with previous reports. Also, to confirm multipotency capacity, ASCs were cultured in osteogenic and adipogenic medium. After culturing the ASCs in osteogenic medium the mineralization of calcium was detected by Alizarin Red S staining (Fig. 1C). Also, following adipogenic differentiation, the accumulation of intracellular lipid vacuole accumulation was detected by Oil Red O staining (Fig. 1D)

Characterization of ANA

According to result, the color of prepared ANA was white and transparent. The elasticity of ANA was lower than fresh nerves, but the diameter and length were slightly decreased compared with normal nerves. H&E staining (Fig. 2) and DAPI staining (Fig. 3) showed that axon, myelin sheath, and cells nuclei were disappeared in decellularized nerves and the basement membrane arranged in a wave-like manner. Normal nerve exhibited intact axons and the myelin sheath was mesh-like with faint staining. Schwann cell could be seen as deep blue in the normal nerves (Fig. 2 A, B).

JPET Fast Forward. Published on December 27, 2018 as DOI: 10.1124/jpet.118.254540
This article has not been copyedited and formatted. The final version may differ from this version.

Also, the removal of myelin was evaluated by toluidine blue staining tissue sections for lipids. Photographs showed that the normal nerve showed regular topography, well myelinated axons of varying diameter (Fig. 4 A, B). But myelinated axons were disappeared in ANA sections (Fig. 4 C, D). Moreover, SEM micrograph revealed that 3D structures of ANA were preserved at an acceptable level. Micrograph showed that the morphology of the ANA changed partly after chemical decellularization process (Fig. 5B, C).

Tensile testing of ANA

Peripheral nerve trunks are viscoelastic tissues with unique mechanical characteristics. Tensile testing was performed to determine the difference in tensile strength between fresh and decellularized peripheral nerve. There were no differences in the average lengths and widths of the specimens. Result showed that the mean ultimate stress, ultimate load and breaking stress for ANA decreased compared with average for intact nerve, significantly. Albeit satisfactorily strong for reconstructive methodology, the tensile strength of ANA had diminished in comparison with fresh nerve (Table 1).

Biocompatibility

ANA biocompatibility assay was performed for evaluating cells retention capacity of ANA before in vivo implantation. After 4 h incubation of ASCs-ANA constructs, SEM micrographs showed that cells adhered well to the ANA (Fig. 5C-D). SEM micrographs showed that ASCs were evenly distributed in the basilar membrane of ANA. After culturing for 96 h, MTT assay result showed that cell viability and proliferation was not significantly different among ASCs were seeded on ANA and ASCs were cultured in 96 well plates at 24 and 48 h. With increasing culture time, cell proliferation rate of control group was significantly higher than ASCs-ANA construct group at 72 and 96 h. These result indicated that ANA had no toxic effects on implanted ASCs, after culturing for 96 h. The data are expressed as the ratio of the mean of OD of the treated groups to that of the control group ($P < 0.05$; Fig. 6).

Functional evaluation

Behavioral analysis was performed to to evaluate motor and sensory function recovery. All animals survived and recovered from anaesthesia. No surgical complications occurred except autotomy of the experimental foot following sciatic nerve axotomy. Autotomy was detected in two animals from the ANA group, one animal from autograft group and one animal from ANA+ASCs group. Autotomy leads to premature euthanasia of the animals using CO_2 inhalation. Also, no side-effects were observed as a result of the two weeks daily i.p injection of ALCAR. The recovery of locomotive function in rats was evaluated by calculating the SFI. The SFI value varies from 0 to -100, with corresponding to the normal function and -100 corresponding to complete dysfunction. The mean SFI value in all groups was approximately (-5 ± 0.78) before surgery, indicating normal function. At postoperative 4 week, the SFI values in all experimental groups decreased dramatically to the lowest level with no obvious difference, indicating complete loss of function. At postoperative 8, 12 and 16 weeks, the SFI value in autograft group and ALCAR treated ASCs–ANA construct groups showed the greatest improvement than other groups, significantly ($p < 0.05$). According to result, SFI value between autograft group and ALCAR treatment ASCs–ANA construct groups was not statistically significant at 16 week postoperative (Fig. 7). Also, the hot plate test was carried out to assess the thermal nociceptive threshold in all groups. Figure 8 show the data for the WRL tests. In the 4^{th} week post-surgery, all animals presented severe loss of sensory function and all tests had to be interrupted at the selected cut off time of 12 s. Nociception recovered significantly along the following weeks except in the negative control group. The results indicated significant differences between groups in the recovery of nociception. According to result, WRL value between autograft group and ALCAR treatment ANA groups was not statistically significant at 16 week postoperative. However, at postoperative 16 week, the WRL value in ALCAR treated ASCs–ANA construct groups showed the greater recovery than autograft group, significantly ($p < 0.05$).

Electrophysiological evaluation

Electrophysiological test was performed for quantitative measurement of electrical motor nerve activity and muscle reinnervation. According to results, the CMAPs amplitude increased and CMAPs onset latencies decreased progressively with time in all groups. NCV were calculated based on CMAP onset latency and the distance between the recording and stimulating electrode tips.The results indicated that ALCAR treatment ASCs–ANA construct group and autograft group achieved significantly higher CMAP peak amplitude, shorter onset latency and higher NCV than other experimental groups at postoperative 16 weeks ($p < 0.05$; Fig. 9). However, the CMAP peak amplitude and NCV for the ALCAR treatment groups was significantly lower than for the sham group ($p < 0.05$). At postoperative 16 weeks, the CMAPs amplitude increased and CMAPs onset latencies of regenerated nerves in the ALCAR treated ASCs–ANA construct groups were similar to that in the autologous nerve group.

Histomorphometry analysis

Morphometric analysis of regenerated sciatic nerves was performed to quantitative estimation of myelinated nerve fiber number and fiber size parameters. In this regards, toluidine blue stained semi-thin transverse sections of distal regenerated nerve stumps were examined by optical microscopy (Fig. 10). Table 2 shows quantitative morphometric analyses of regenerated nerves for each of the experimental groups. At the end of 16-week postoperative, morphometric parameters including total myelinated fiber number, myelin thickness, axon diameter and axonal density were significantly greater in autograft and ALCAR treated ASCs–ANA construct groups compared to other groups, except control ($P < 0.001$). However, the total myelinated fiber number in the ALCAR treated ASCs–ANA construct group was significantly greater than autograft ($p < 0.05$), while no significant difference was found between the ALCAR treatment ANA group and autograft group. Moreover, myelin thickness in the ALCAR treatment ANA group was greater than ASCs–ANA group, significantly ($P < 0.05$). But, it was significantly inferior when compared with to the autograft and ALCAR treated ASCs–ANA construct groups ($P < 0.05$). There were no significant differences between the results of autograft and ALCAR treated ASCs–ANA construct

groups at 16 weeks postoperative. Also, the fiber diameter in the autograft and ALCAR treated ASCs–ANA construct groups was significantly greater than other experimental grous ($P < 0.05$), while no significant difference was found between two group.

Muscle mass and morphology

Sciatic nerve transection produces the loss of the neural innervation to the gastrocnemius muscle, which leads to a decrease in the muscle mass. Therefore, muscle weight was measured to assess denervation atrophy at the end of experiment. According to results, the experimental gastrocnemius muscles exhibited atrophy compared with the contralateral side in all groups. At 16 weeks after surgery, the muscle weight showed a recovery up to 54.1±0.5% in the autograft group and 58.3±0.6% in the ALCAR treated ASCs–ANA construct group. Also, the results showed that muscle mass ratio was higher in the ALCAR treatment ANA groups than ASCs–ANA construct and ANA groups. These results indicated that gastrocnemius muscle atrophy was reduced by systemic administration of ALCAR. No significant difference was observed between the ALCAR treatment ASCs–ANA construct and autograft group (Fig. 11).

RT-PCR

Schwann cells and neurotrophic factors are keys factors in nerve regeneration process. In this regards, nerve grafts were subjected to qRT-PCR to evaluate the mRNA levels of neurotrophin (NGF, GDNF and BDNF) genes and Schwann cell lineage-related genes (S100 and p75) at 2-week postoperative .Results showed that ALCAR treated ASCs–ANA construct group expressed a wide range of neurotrophin genes. According to result, NGF, BDNF and GDNF were significantly upregulated in both autograft group and ALCAR treated ASCs–ANA construct group ($P < 0.01$; Fig. 12). Importantly, there was significant difference between the ALCAR treated ASCs–ANA construct group and ASCs–ANA construct in term of NGF and GDNF gene expression ($P < 0.01$; Fig. 12). Also, the pattern of gene expression for key markers of the Schwann cell lineage (S100 and p75) was compared in all groups. RT-PCR analysis indicated that Schwann cell markers

mRNA were significantly upregulated in ALCAR treated ASCs–ANA construct group in comparison with ASCs–ANA construct group and ALCAR treated ANA group ($P < 0.001$; Fig. 12). This finding suggests that the number of Schwann cells increased in ALCAR treated ASCs–ANA construct group. Moreover, our result showed that ALCAR treatment decreased Caspase 3 mRNA expression at the site of nerve injury in ANA-ASCs construct engrafted rat.

Discussion

Acellular nerve allograft is a good alternative for autograft. However, animal research indicated that regenerative effect of acellular nerve allograft was still lower than autograft due to the lack of an appropriate microenvironment for axonal regeneration. It seems that implanted ASCs could improve microenvironment of ANA through secretion of neurotrophins and growth factors (Y. Zhang et al., 2010). However, transplanted ASCs encounter an ischemic microenvironment characterized by hypoxia, serum and nutrition deprivation (Potier et al., 2007). Metabolic stress is a main cause of limitation for ASCs viability after transplantation and short lifespan of transplanted ASCs limits their therapeutic efficacy (Chavakis, Urbich, & Dimmeler, 2008; Potier et al., 2007). It's well known that the efficacy of cell therapy will depend on the possibility of delivering a large number of viable functional cells into injured tissue (Potier et al., 2007). Therefore, we hypothesized that administration of ALCAR as a neuroprotective and antiapoptotic substance may be a way to increase survival rate and retention of transplanted ASCs under stressful conditions at injury site. ALCAR is a short chain ester of carnitine l-isomer that plays an important role in long-chain fatty acid transport across the mitochondrial membrane for β-oxidation and ATP production (Bak et al., 2016; Hart, Wiberg, & Terenghi, 2002). Also, it protects cells against lipid peroxidation and mitochondrial membrane breakdown through its anti-oxidative activity (Gülçin, 2006; Tesco et al., 1992; R. Zhang et al., 2012). Therefore, we evaluated the effect of ALCAR treatment (50 mg/kg/day) on the efficiency of acellular nerve graft for repair of the 10 mm gap in rat sciatic nerve. For this study, dose of 50 mg/kg was chosen as this dose provided the significant improvement in nerve regeneration process (Wilson, Hart,

Wiberg, & Terenghi, 2010). For this purpose, we employed ANA, ANA supplemented with ASCs and autograft as a control for reconstruction of nerve defect. No signs of rejection and infection were observed. Our result showed that ANA provided three-dimension scaffold that supports axonal regeneration and muscle reinnervation. Result indicated that transplanted ASCs could significantly improve regenerative properties of acellular nerve graft in comparison with acellular nerve graft group at the end of experiment. But, its therapeutic capacity was still inferior to autograft group which is in agreement with other studies (Scheib & Höke, 2013). Therefore, ALCAR treatment led to improvement of regenerative properties of ASCs supplemented ANA. ALCAR treatment led to significant improvement of locomotion recovery (as indexed by the SFI value) in ASCs supplemented ANA groups in comparision with untreated groups. However, no significant difference was observed in comparison with autograft. Also, results indicated that ALCAR treatment attenuated muscle mass loss during organ denervation. Electrophysiological assessment provided further evidence that the nerve regeneration in autograft group and ALCAR treated ASCs supplemented ANA groups was significantly superior to other groups. Furthermore, histological evaluation showed that in autograft group and ALCAR treated allograft groups, more axons successfully crossed the graft from proximal to the distal segment. ALCAR treated allograft groups and autograft group exhibited better reconstruction of regenerated nerve and the gastrocnemius target muscle than other groups. These data demonstrated that the systemic administration of ALCAR enhanced ASCs transplanted nerve allograft regenerative properties and consequence peripheral nerve regeneration. The mechanism of the action of the ASCs has not been definitively elucidated but some studies suggest that they work by either releasing growth factors themselves or by modulating the endogenous Schwann cells (Lopatina et al., 2011). Regeneration of nerve injury depends on interaction between SCs and regenerative axons. SCs ability for the secretion of neurotrophic factors (such as NGF, GDNF and BDNF) plays an important role in successful neural recovery (Elgazzar, Mutabgani, Abdelaal, & Sadakah, 2007). Our result showed that ALCAR treatment allograft supplemented with ASCs groups and autograft group expressed

SCs marker (S100, P75) and neurotrophic factors (NGF, GDNF and BDNF). The mRNA levels of NGF and BDNF were similar between ALCAR treatment allograft supplemented with ASCs group and the autograft group. Neurotrophins have been shown to improve neuronal survival and nerve regeneration in nerve injuries (Tang et al., 2013). The release neurotrophins into acellular nerve grafts might contribute to the establishment of a native-like microenvironment for nerve regeneration in a similar manner to autografts. These factors may have partly originated from the ASCs that embedded in ANA or ASCs derived SCs like cells. Some evidences indicated that ASCs could differentiation to Schwann cell-like cells that expressed Schwann cell markers (Kingham et al., 2007). In vitro studies showed that differentiated ASCs enhance neurite outgrowth (Jiang et al., 2008) and this has been attributed to elevated levels of NGF and BDNF (Kingham et al., 2007). Therefore, we concluded that ALCAR treatment resulted in improve regenerative properties of cell seeded nerve allograft likely via increasing transplanted ASCs viability and retention. However, the precise mechanism by which ALCAR improved nerve regeneration remains to be determined. It seems that ALCAR treatment could improve survival rate and retention of ASCs embedded in ANA and also improve peripheral nerve regeneration and functional recovery. Studies showed that Schwann cells and ASCs death occurs under ischemic conditions (Keilhoff, Schild, & Fansa, 2008). Some studies showed that ALCAR treatment has protective effect against stress induced apoptosis in cultured cells (Ishii, Shimpo, Matsuoka, & Kinoshita, 2000; Pillich, Scarsella, & Risuleo, 2005). In agreement with these finding, our unpublished results showed that ALCAR (10 mM) treatment attenuated serum and glucose deprivation induced apoptosis in cultured rat ASCs. Similarly, Fujisawa and coworker confirmed that L-carnitine suppresses Doxorubicin induced apoptosis in bone marrow MSCs. Evidences indicated that ALCAR may prevent failure of mitochondrial oxidative metabolism (Altamimi et al., 2018) (Bak et al., 2016). In vitro studies demonstrated that ALCAR was able to attenuate the rate of neuronal mortality (Manfridi, Forloni, Arrigoni-Martelli, & Mancia, 1992). Also, in vivo studies indicated that ALCAR has a protective effect on peripheral nerve injuries (Fernandez et al.,

1989) (Hart, Wiberg, Youle, et al., 2002). In this regard, it has been shown that ALCAR prevented sensory neuronal loss after axotomy by enhancing mitochondrial bioenergetics function (Hart, Wiberg, Youle, et al., 2002). Some studies indicated that after nerve injury, ALCAR could attenuate mitochondrial oxidative stress and consequence mitochondrial induced cell death by reduced cytosolic levels of cytochrome-C and caspase-3 active fragments (Di Cesare Mannelli et al., 2007). In accordance with these finding, our result showed that ALCAR treatment decreased Caspase 3 mRNA expression at the site of nerve injury in ANA-ASCs construct engrafted rat. Previous results showed that ALCAR treatment increase NGF responsiveness by enhancing the expression and affinity of neurotrophin receptors for NGF (Taglialatela et al., 1991)(Manfridi et al., 1992). Taken together, these findings suggest that ALCAR may be an effective neuroprotective agent for peripheral nerve regeneration that could improve the therapeutic efficacy of transplanted ASCs–ANA constructs.

Conclusion: In conclusion, our results showed that co-application of acellular grafts incorporating ASCs as tissue-engineered ANA and ALCAR administration represent promising treatments for the repair of peripheral nerve large defects. This method can be a good and easily adapted to most clinical settings. Future studies should be done to confirm the precise mechanism of ALCAR function.

Acknowledgement

The authors would like to thank Dr. Ann Paterson for assisting with English.

Conflict of interest: The authors declare that they have no conflict of interest.

Authorship Contributions:

Participated in research design: Ghayour, Behnam-Rassouli, Abdolmaleki

Conducted experiments: Ghayour, Abdolmaleki

Performed data analysis: Mahdavi-Shahri Naser, Ghayour, Abdolmaleki

Wrote or contributed to the writing of the manuscript: Ghayour, Abdolmaleki**,** Moghimi

References

Altamimi TR, Thomas PD, Darwesh AM, Fillmore N, Mahmoud MU, Zhang L, Lopaschuk G (2018) Cytosolic carnitine acetyltransferase as a source of cytosolic acetyl-CoA: a possible mechanism for regulation of cardiac energy metabolism. *Biochemical Journal* BCJ20170823.

Bak SW, Choi H, Park HH, Lee KY, Lee YJ, Yoon MY, Koh SH (2016) Neuroprotective effects of acetyl-L-carnitine against oxygen-glucose deprivation-induced neural stem cell death. *Molecular neurobiology 53*(10): 6644-6652.

Brohlin M, Mahay D, Novikov LN, Terenghi G, Wiberg M, Shawcross SG, Novikova LN (2009) Characterisation of human mesenchymal stem cells following differentiation into Schwann cell-like cells. *Neuroscience research 64*(1): 41-49.

Chavakis E, Urbich C, Dimmeler S (2008) Homing and engraftment of progenitor cells: a prerequisite for cell therapy. *Journal of molecular and cellular cardiology 45*(4): 514-522.

Di Cesare Mannelli L, Ghelardini C, Calvani M, Nicolai R, Mosconi L, Vivoli E, Bartolini A (2007) Protective effect of acetyl‐l‐carnitine on the apoptotic pathway of peripheral neuropathy. *European Journal of Neuroscience 26*(4): 820-827.

di Summa PG, Kalbermatten DF, Pralong E, Raffoul, W, Kingham PJ, Terenghi G (2011) Long-term in vivo regeneration of peripheral nerves through bioengineered nerve grafts. *Neuroscience 181*: 278-291.

Dijkstra JR, Meek MF, Robinson PH, Gramsbergen A (2000) Methods to evaluate functional nerve recovery in adult rats: walking track analysis, video analysis and the withdrawal reflex. *Journal of neuroscience methods 96*(2): 89-96.

Doolabh VB, Hertl MC, Mackinnon SE (1996) The role of conduits in nerve repair: a review. *Reviews in the Neurosciences 7*(1): 47-84.

Elgazzar R, Mutabgani M, Abdelaal S, Sadakah A (2007) Platelet-rich plasma may enhance peripheral nerve regeneration after cyanoacrylate reanastomosis: a randomized blind study on rats. *International Journal of Oral and Maxillofacial Surgery 36*(11): 1031.

Fernandez E, Pallini R, Gangitano C, Del Fá A, Sangiacomo CO, Sbriccoli A, Rossi GF (1989) Effects of L-carnitine, L-acetylcarnitine and gangliosides on the regeneration of the transected sciatic nerve in rats. *Neurological research: 11*(1): 57-62.

Ghayour MB, Abdolmaleki A, Behnam-Rassouli M (2016) The effect of Riluzole on functional recovery of locomotion in the rat sciatic nerve crush model. *European Journal of Trauma and Emergency Surgery* 1-9.

Gimble JM, Katz AJ, Bunnell BA (2007) Adipose-derived stem cells for regenerative medicine. *Circulation research 100*(9): 1249-1260.

Gülçin İ (2006) Antioxidant and antiradical activities of L-carnitine. *Life sciences 78*(8): 803-811.

Hargreaves K, Dubner R, Brown F, Flores C, Joris J (1988) A new and sensitive method for measuring thermal nociception in cutaneous hyperalgesia. *Pain 32*(1): 77-88.

Hart AM, Wiberg M, Terenghi G (2002) Pharmacological enhancement of peripheral nerve regeneration in the rat by systemic acetyl-L-carnitine treatment. *Neuroscience letters 334*(3): 181-185.

Hart AM, Wiberg M, Youle M, Terenghi G (2002) Systemic acetyl-L-carnitine eliminates sensory neuronal loss after peripheral axotomy: a new clinical approach in the management of peripheral nerve trauma. *Experimental brain research 145*(2): 182-189.

Ishii T, Shimpo Y, Matsuoka Y, Kinoshita K (2000) Anti-apoptotic effect of acetyl-L-carnitine and L-carnitine in primary cultured neurons. *The Japanese Journal of Pharmacology 83*(2): 119-124.

Jessen KR, Mirsky R (2008) Negative regulation of myelination: relevance for development, injury, and demyelinating disease. *Glia 56*(14): 1552-1565.

Jiang L, Zhu JK, Liu XL, Xiang P, Hu J, Yu WH (2008) Differentiation of rat adipose tissue-derived stem cells into Schwann-like cells in vitro. *Neuroreport 19*(10): 1015-1019.

Keilhoff G, Schild L, Fansa H (2008) Minocycline protects Schwann cells from ischemia-like injury and promotes axonal outgrowth in bioartificial nerve grafts lacking Wallerian degeneration. *Experimental neurology 212*(1): 189-200.

Kingham PJ, Kalbermatten DF, Mahay D, Armstrong SJ, Wiberg M, Terenghi G (2007) Adipose-derived stem cells differentiate into a Schwann cell phenotype and promote neurite outgrowth in vitro. *Experimental neurology 207*(2): 267-274.

Kokai LE, Rubin JP, Marra KG (2005) The potential of adipose-derived adult stem cells as a source of neuronal progenitor cells. *Plastic and reconstructive surgery 116*(5): 1453-1460.

Kuroda Y, Kitada M, Wakao S, Nishikawa K, Tanimura Y, Makinoshima H, Niwa A (2010) Unique multipotent cells in adult human mesenchymal cell populations. *Proceedings of the National Academy of Sciences 107*(19): 8639-8643.

Locke M, Windsor J, Dunbar P (2009) Human adipose‐derived stem cells: isolation, characterization and applications in surgery. *ANZ journal of surgery 79*(4): 235-244.

Lopatina T, Kalinina N, Karagyaur M, Stambolsky D, Rubina K, Revischin A, Tkachuk V (2011) Adipose-derived stem cells stimulate regeneration of peripheral nerves: BDNF secreted by these cells promotes nerve healing and axon growth de novo. *PloS one 6*(3): e17899.

Lu Q, Zhang Y, Elisseeff JH (2015) Carnitine and acetylcarnitine modulate mesenchymal differentiation of adult stem cells. *Journal of tissue engineering and regenerative medicine 9*(12): 1352-1362.

Mackinnon SE, Hudson AR (1992) Clinical application of peripheral nerve transplantation. *Plastic and reconstructive surgery 90*(4): 695-699.

Manfridi A, Forloni GL, Arrigoni-Martelli E, Mancia M (1992) Culture of dorsal root ganglion neurons from aged rats: effects of acetyl-L-carnitine and NGF. *Int J Dev Neurosci 10*(4): 321-329.

Mansour HH (2006) Protective role of carnitine ester against radiation-induced oxidative stress in rats. *Pharmacological research 54*(3): 165-171.

McKenzie JL, Gan OI, Doedens M, Wang JC, Dick JE (2006) Individual stem cells with highly variable proliferation and self-renewal properties comprise the human hematopoietic stem cell compartment. *Nature immunology 7*(11): 1225-1233.

Mosahebi A, Fuller P, Wiberg M, Terenghi G (2002) Effect of allogeneic Schwann cell transplantation on peripheral nerve regeneration. *Experimental neurology 173*(2): 213-223.

Navarro X, Udina E (2009) Methods and protocols in peripheral nerve regeneration experimental research: part III—electrophysiological evaluation. *International review of neurobiology 87*: 105-126.

Neubauer D, Graham JB, Muir D (2010) Nerve grafts with various sensory and motor fiber compositions are equally effective for the repair of a mixed nerve defect. *Experimental neurology 223*(1): 203-206.

Oğğuzhanoğğlu A, Erdoğğan Ç, Tabak E, Cenikli U (2010) Comparison of conduction velocities of nerve fibers to smaller and larger muscles in rats. *International Journal of Neuroscience 120*(1): 76-79.

Pillich RT, Scarsella G, Risuleo G (2005) Reduction of apoptosis through the mitochondrial pathway by the administration of acetyl-L-carnitine to mouse fibroblasts in culture. *Experimental cell research 306*(1): 1-8.

Potier E, Ferreira E, Meunier A, Sedel L, Logeart-Avramoglou D, Petite H (2007) Prolonged hypoxia concomitant with serum deprivation induces massive human mesenchymal stem cell death. *Tissue engineering 13*(6): 1325-1331.

Raimondo S, Fornaro M, Di Scipio F, Ronchi G, Giacobini‐Robecchi MG, Geuna S (2009) Methods and protocols in peripheral nerve regeneration experimental research: part II—morphological techniques. *International review of neurobiology 87*: 81-103.

Scheib J, Höke A (2013) Advances in peripheral nerve regeneration. *Nature Reviews Neurology 9*(12): 668.

Siemionow M, Bozkurt M, Zor F (2010) Regeneration and repair of peripheral nerves with different biomaterials: review. *Microsurgery 30*(7): 574-588.

Sondell M, Lundborg G, Kanje M (1998) Regeneration of the rat sciatic nerve into allografts made acellular through chemical extraction. *Brain research 795*(1): 44-54.

Taglialatela, G., Angelucci, L., Ramacci, M., Werrbach-Perez, K., Jackson, G., & Perez-Polo, J. (1991). Acetyl-L-carnitine enhances the response of PC12 cells to nerve growth factor. *Developmental brain research, 59*(2), 221-230.

Tang S, Zhu J, Xu Y, Xiang AP, Jiang MH, Quan D (2013) The effects of gradients of nerve growth factor immobilized PCLA scaffolds on neurite outgrowth in vitro and peripheral nerve regeneration in rats. *Biomaterials 34*(29): 7086-7096.

Tesco G, Latorraca S, Piersanti P, Piacentini S, Amaducci L, Sorbi S (1992) Protection from oxygen radical damage in human diploid fibroblasts by acetyl-L-carnitine. *Dementia and Geriatric Cognitive Disorders 3*(1): 58-60.

Tohill M, Terenghi G (2004) Stem ‐ cell plasticity and therapy for injuries of the peripheral nervous system. *Biotechnology and applied biochemistry 40*(1): 17-24.

Toma C, Pittenger MF, Cahill KS, Byrne BJ, Kessler PD (2002) Human mesenchymal stem cells differentiate to a cardiomyocyte phenotype in the adult murine heart. *Circulation 105*(1): 93-98.

Wilson AD, Hart A, Wiberg M, Terenghi G (2010) Acetyl-l-carnitine increases nerve regeneration and target organ reinnervation–a morphological study. *Journal of Plastic, Reconstructive & Aesthetic Surgery 63*(7): 1186-1195.

Zhang R, Zhang H, Zhang Z, Wang T, Niu J, Cui D, Xu S (2012) Neuroprotective effects of pre-treament with l-carnitine and acetyl-l-carnitine on ischemic injury in vivo and in vitro. *International journal of molecular sciences 13*(2): 2078-2090.

Zhang Y, Luo H, Zhang Z, Lu Y, Huang X, Yang L, Du B (2010) A nerve graft constructed with xenogeneic acellular nerve matrix and autologous adipose-derived mesenchymal stem cells. *Biomaterials 31*(20): 5312-5324.

Table legends

Table 1. Tensile Testing of Acellular Nerve and Normal Sciatic Nerves (n=10).

Table 2. Morphometric analyses of transverse sections at the sciatic nerve distal to injury for each of the experimental groups 16 weeks post-injury. Values are shown as mean ± SD. * $P < 0.05$, ** $P < 0.01$ and ***$P < 0.001$ vs. autograft group.

Figure legends

Figure 1. Flow cytometry characterization and multipotency confirmation of ASCs obtained from adult male Wistar rats**.** (**A**) Flow cytometry results demonstrated that ASCs at passage 3 were uniformly negative for CD11b, CD31 and CD45 and positive for CD29 and CD90 expression. (**B**) Isolated ASCs showed fibroblast-like shapes (B), and exhibited multi-differentiation capacity osteogenic and adipogenic differentiation respectively (C and D).

Figure 2. Hematoxylin-eosin staining was used to compare the general morphology of fresh rat sciatic nerve to acellular nerve allograft (Sondell protocol). (A and C) represent cross-section of intact nerve and acellular nerve respectively. (B and D) represent longitudinal-section of intact nerve and acellular nerve respectively. The schwann cell nuclei were stained in deep blue (arrowhead) and the myelin sheaths were mesh-like with faint staining in fresh nerve segment. Arrows represent the nerve fibers (axons and myelin sheaths). But, in ANA, axons and cell nuclei were disappeared.

Figure 3. DAPI stained cross-section of rat sciatic nerve were used to compare the cell's nucleuses of (A) freshly dissected nerve to (B) decellularized nerve segment. Results showed that the cell's nucleuses were disappeared in decellularized nerve.

ANA cross-section were stained with DAPI and immediately viewed under fluorescence microscopy. (A) Control segment from freshly dissected nerve. (B) Cross section from nerve segment after decellularization.

Figure 4. Toluidine blue staining was conducted on samples of the acellular nerve to confirm decellularization process. (A and C) Cross-section of fresh nerve and acellular nerve Cross-section, respectively. (B and D) Longitudinal section of fresh nerve and acellular nerve, respectively. Myelin sheath and axon were disappeared in acellular nerve segment.

Figure 5. Scanning electron microscopy of longitudinal nerve and ANA. Longitudinal section of fresh nerve (A) and acelular nerve (B). The 3D structure of acellular nerve was not severely destroyed by decellularization process. After co-culture for 4 h, the cells were adhering to the ANA (C).

Figure 6. Evaluation of ANA biocompatibility. The viability and proliferation of ASCs that seeded on ANA was compared with ASCs were cultured in 96 well plates using MTT assay. MTT assay show that ANA has no toxic effect on cell viability and proliferation under normal culture condition**.** The experiments were performed in triplicate (n=10).

Figure 7. Sciatic function index (SFI) measured every 4 week after surgery in each experimental group. Data were expressed as mean ± SD (n = 10). * $P < 0.05$, ** $P < 0.01$ and ***$P < 0.001$ vs. Autograft group at the same time point.

Figure 8. Withdrawal reflex latency (WRL) test using a hot plate was performed every 4 week after surgery in each experimental group. Data were expressed as mean ± SD (n = 10). * $P < 0.05$, ** $P < 0.01$ and ***$P < 0.001$ vs. autograft group at the same time point.

Figure 9. (A) Representative results of CMAP amplitude measurements after proximal stimulation of operated and unoperated sciatic nerves at 8^{th} and 16^{th} weeks post-surgery. The data are shown as

mean ± SD (n = 10). * P < 0.05 and ***P < 0.001 vs. autograft group. (B) Representative results of CMAP delay measurements at 8^{th} and 16^{th} weeks post-surgery. The data are shown as mean ± SD (n = 10). ** P < 0.01 and ***P < 0.001 vs. autograft group. (C) Representative results of conduction velocity measurements at 8^{th} and 16^{th} weeks post-surgery. The data are shown as mean ± SD (n = 10). ** P < 0.01 and ***P < 0.001 vs. autograft group.

Figure 10. Toluidine blue staining of semithin resin cross-sections of distal sciatic nerve stumps at 16 weeks post-operation. Figure showed myelinated axons in Control (A), Autograft (B), ANA+ASCs+ALCAR (C), ANA+ALCAR (D), ANA+ASCs (E), ANA alone (F) (Scale bar: 50 μm).

Figure 11. Gastrocnemius muscle weight ratio measurement. The gastrocnemius muscles of operated and unoperated sides were excised and weighed in the experimental groups at 16 weeks post-operatively. Graph show mean gastrocnemius muscle weight ratio (experimental/control). The data are shown as mean ± SD (n = 10). ** P < 0.01 and ***P < 0.001 vs. autograft group.

Figure 12. Real-time quantitative RT-PCR analyses of neurotrophin (A), Schwan cell markers (B) and caspase 3 (C) mRNA expression in implanted grafts. The mRNA level in naive rats has been ascribed a value of 1 and the vertical axis numbers indicate relative changes from this baseline for each group. The data are shown as mean ± SEM (n = 6). * P < 0.05, ** P < 0.01 and ***P < 0.001 vs. autograft group.

JPET Fast Forward. Published on December 27, 2018 as DOI: 10.1124/jpet.118.254540
This article has not been copyedited and formatted. The final version may differ from this version.

Table 1

Groups	Peak Force (N)	Ultimate stress (MPa)	Ultimate Strain (%)	Peak Extension (mm)	Break stress (MPa)
Control	**2.04±0.55**	**0.65±0.16**	**42.02±18.12**	**4.22±1.79**	**0.04±0.05**
ANA	**1.35±34***	**0.41±0.11***	**64.33±15.1***	**6.3±1.47***	**0.2±0.15***

Table 2

Groups	Axon diameter	Myelin thickness	Fiber diameter	Myelinated Fiber count	G-Ratio
Control	**4.92±0.31**	**1.35±0.2**	**7.63±0.68**	**7701±1053**	**0.64**
Autograft	**3.55±0.62**	**1.11±0.2**	**5.78±0.74**	**14135±2630**	**0.61**
ANA	**2.41±0.39*****	**0.53±0.16*****	**3.46±0.7*****	**9271±2310*****	**0.7**
ANA+ASCs	**3.02±0.58***	**0.7±0.18*****	**4.42±0.89*****	**11229±1465*****	**0.68**
ANA+ALCAR	**3.1±0.57**	**0.82±0.17****	**4.74±0.22***	**12750±1906**	**0.65**
ANA+ASCs+ALCAR	**3.85±0.46**	**1.04±0.23**	**5.93±0.82**	**16064±1542***	**0.65**

JPET Fast Forward. Published on December 27, 2018 as DOI: 10.1124/jpet.118.254540
This article has not been copyedited and formatted. The final version may differ from this version.

Fig 1

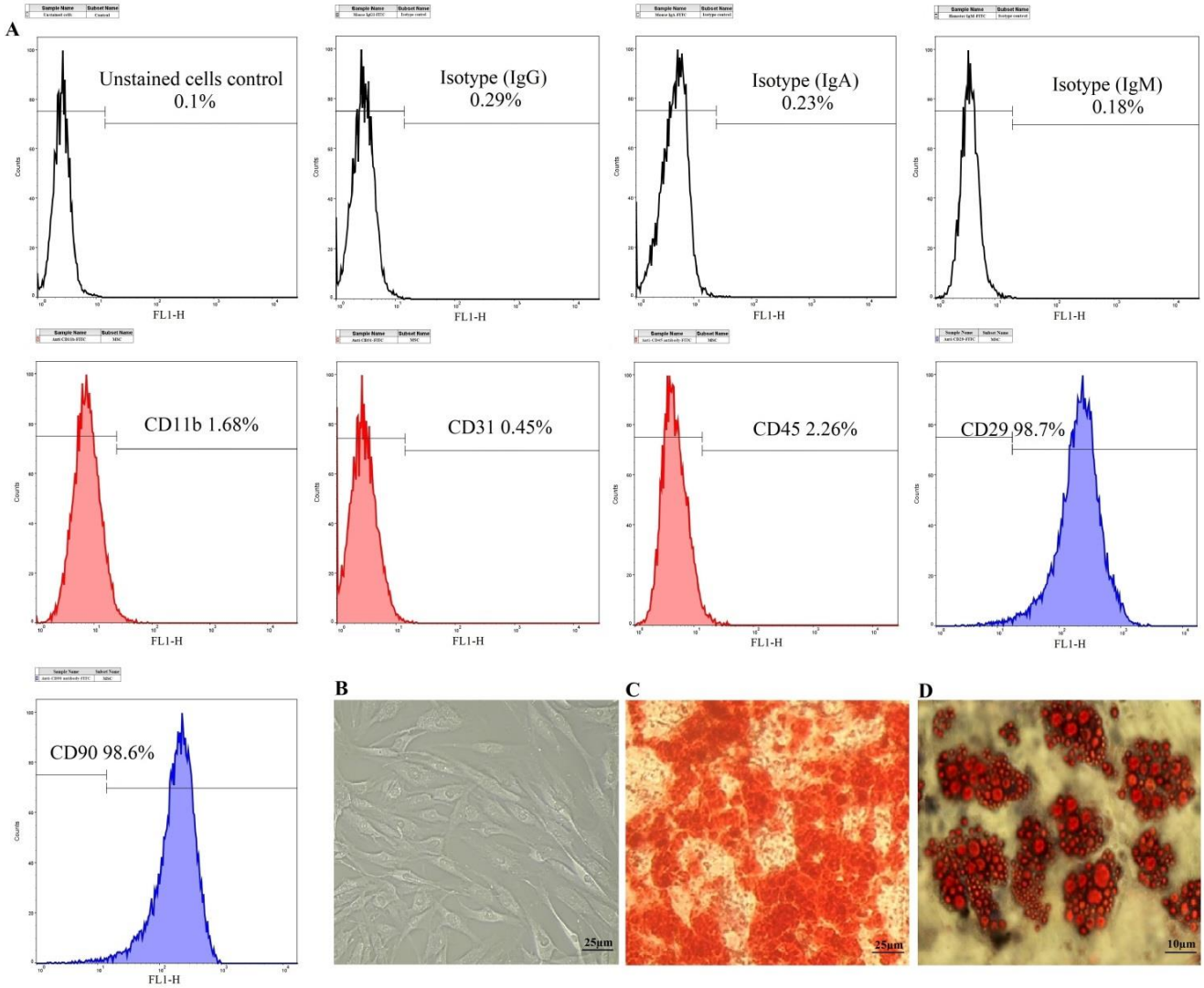

JPET Fast Forward. Published on December 27, 2018 as DOI: 10.1124/jpet.118.254540
This article has not been copyedited and formatted. The final version may differ from this version.

Fig 2

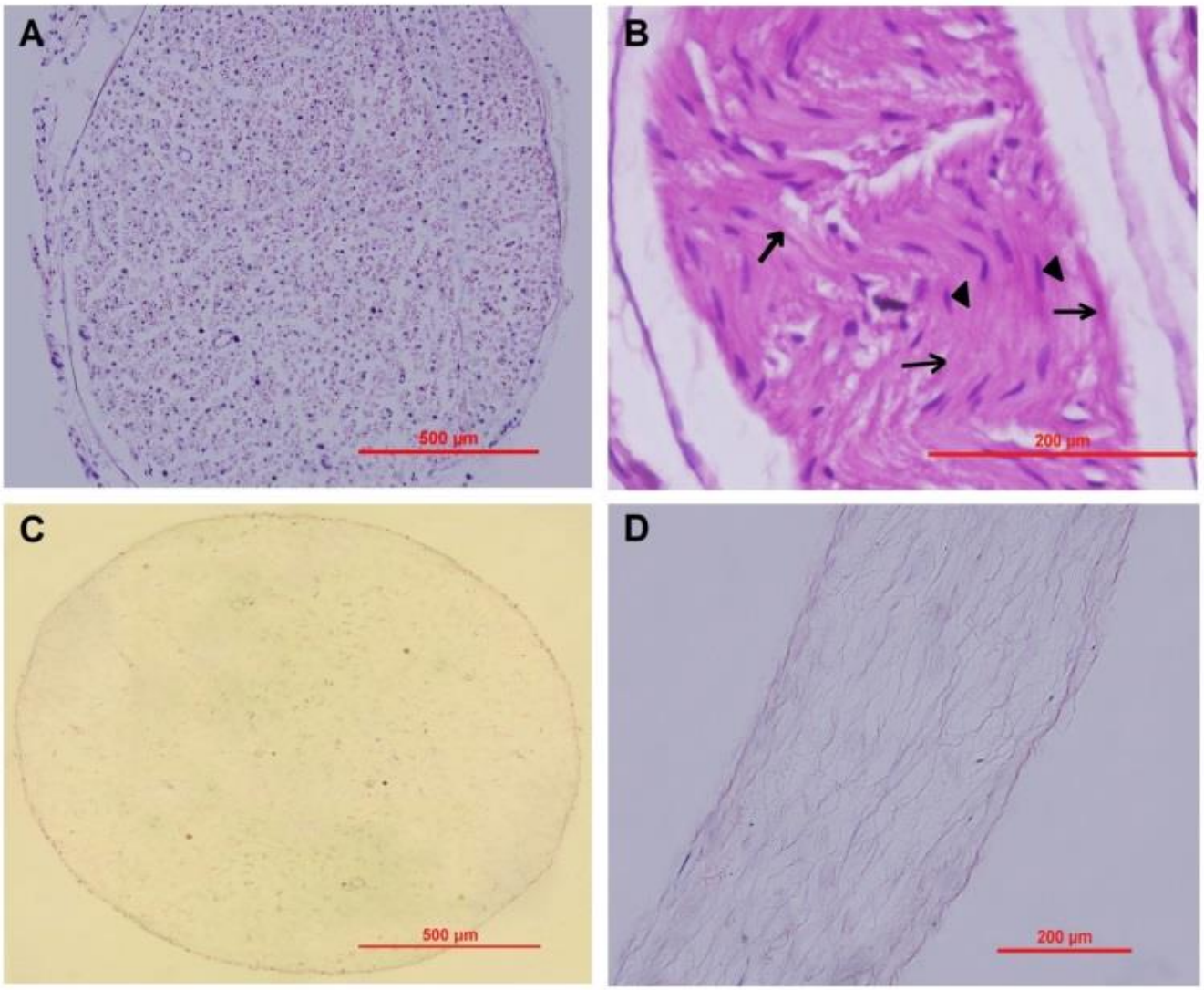

JPET Fast Forward. Published on December 27, 2018 as DOI: 10.1124/jpet.118.254540
This article has not been copyedited and formatted. The final version may differ from this version.

JPET#254540

Fig 3

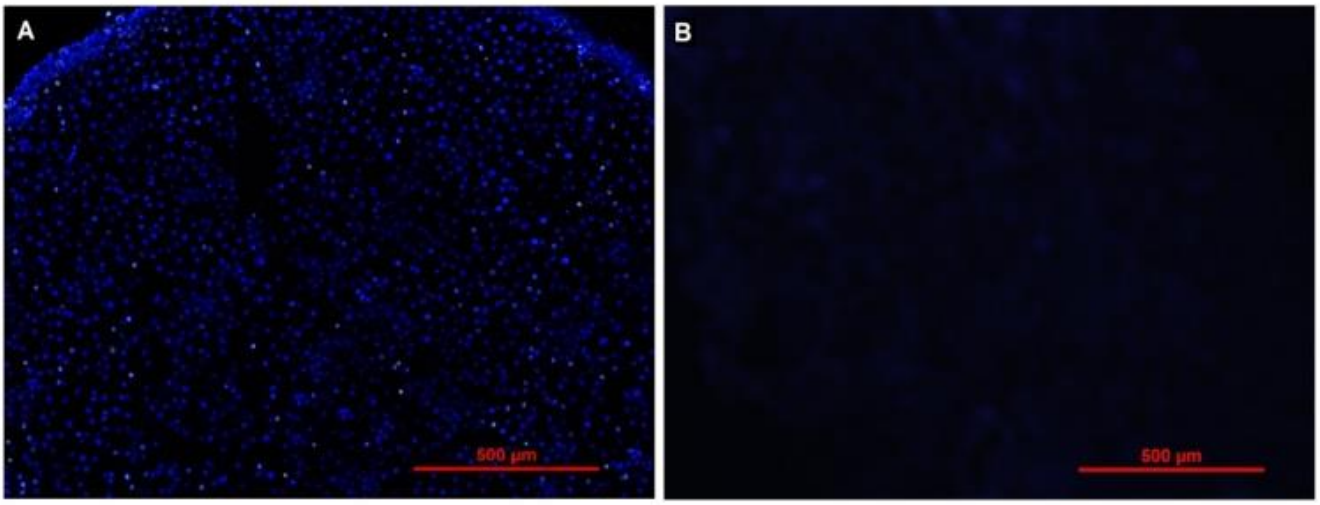

JPET Fast Forward. Published on December 27, 2018 as DOI: 10.1124/jpet.118.254540
This article has not been copyedited and formatted. The final version may differ from this version.

JPET#254540

Fig 4

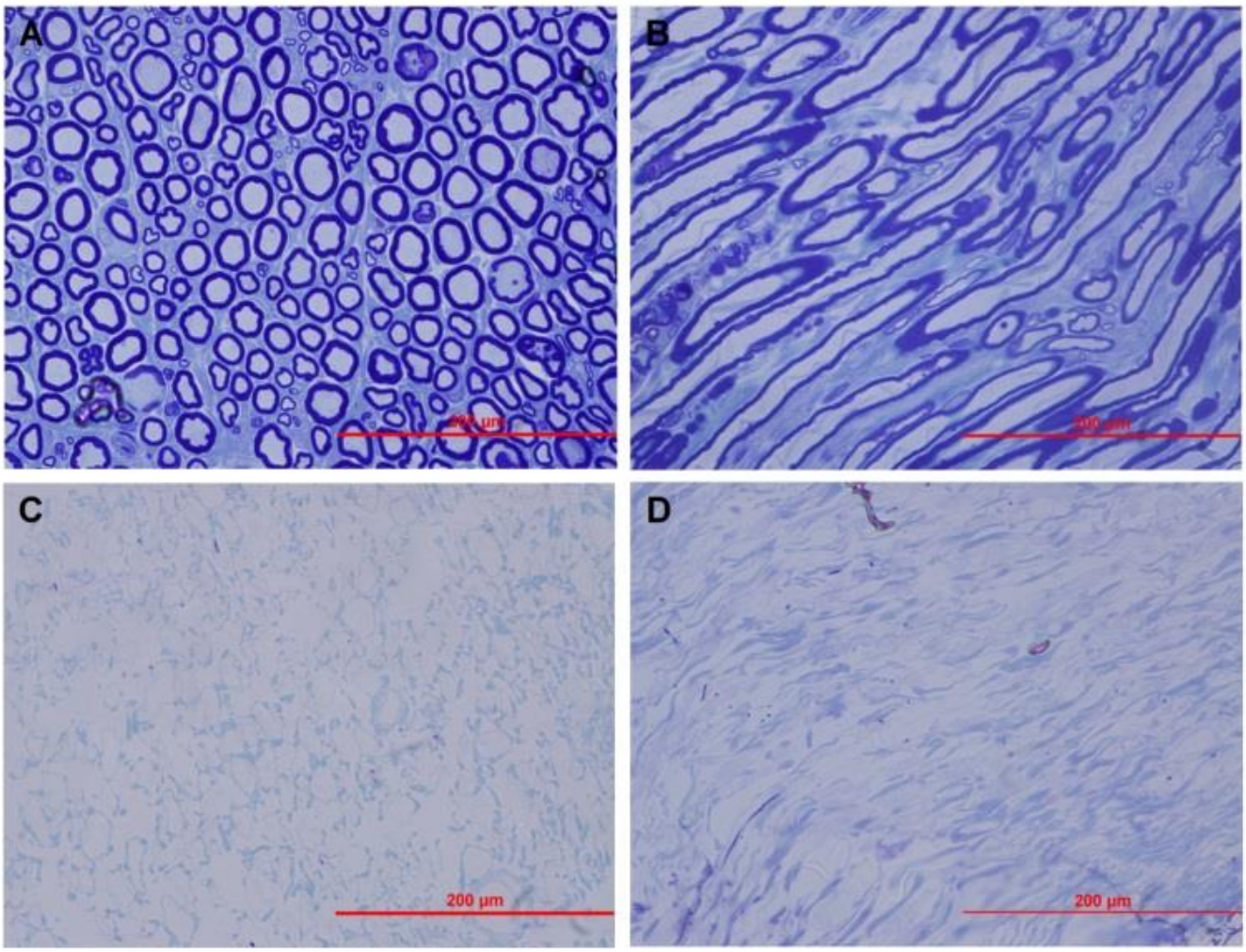

JPET Fast Forward. Published on December 27, 2018 as DOI: 10.1124/jpet.118.254540
This article has not been copyedited and formatted. The final version may differ from this version.

JPET#254540

Fig 5

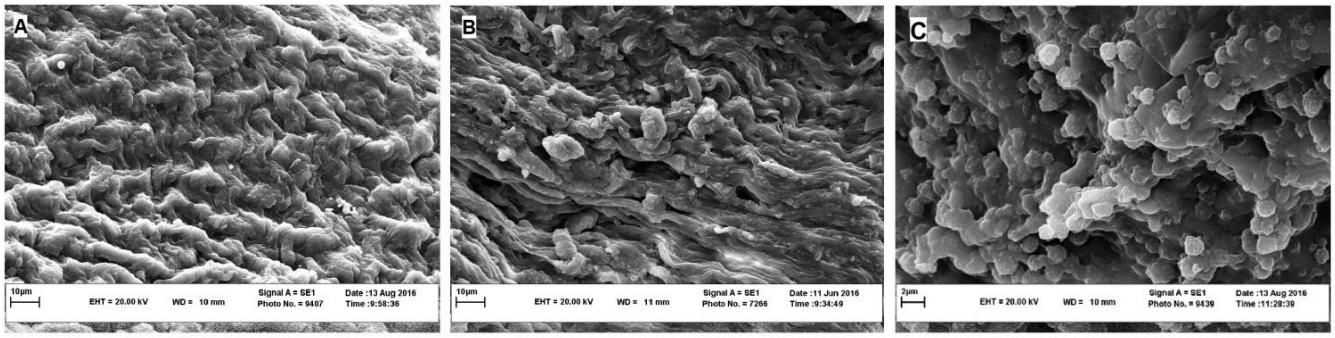

JPET Fast Forward. Published on December 27, 2018 as DOI: 10.1124/jpet.118.254540
This article has not been copyedited and formatted. The final version may differ from this version.

Fig 6

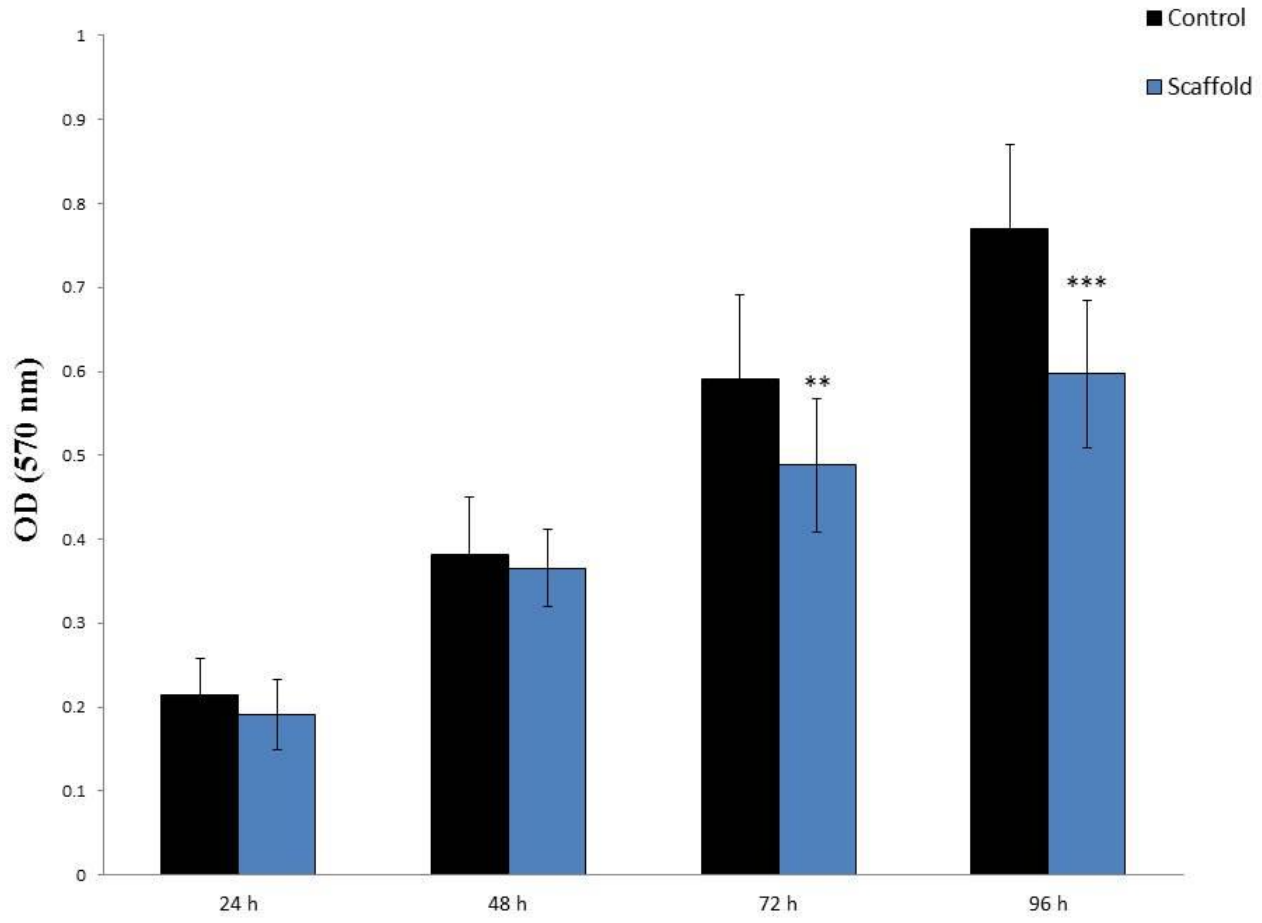

JPET Fast Forward. Published on December 27, 2018 as DOI: 10.1124/jpet.118.254540
This article has not been copyedited and formatted. The final version may differ from this version.

JPET#254540

Fig 7

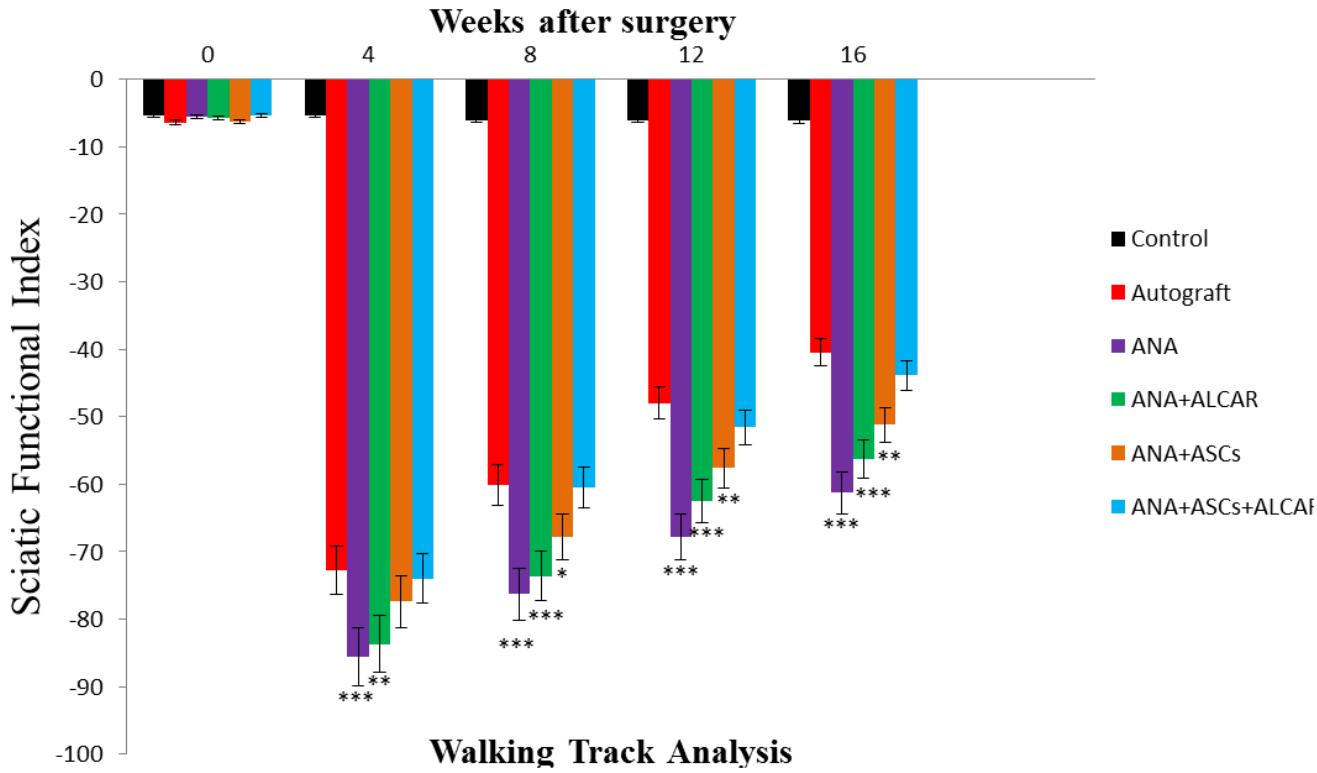

JPET Fast Forward. Published on December 27, 2018 as DOI: 10.1124/jpet.118.254540
This article has not been copyedited and formatted. The final version may differ from this version.

JPET#254540

Fig 8

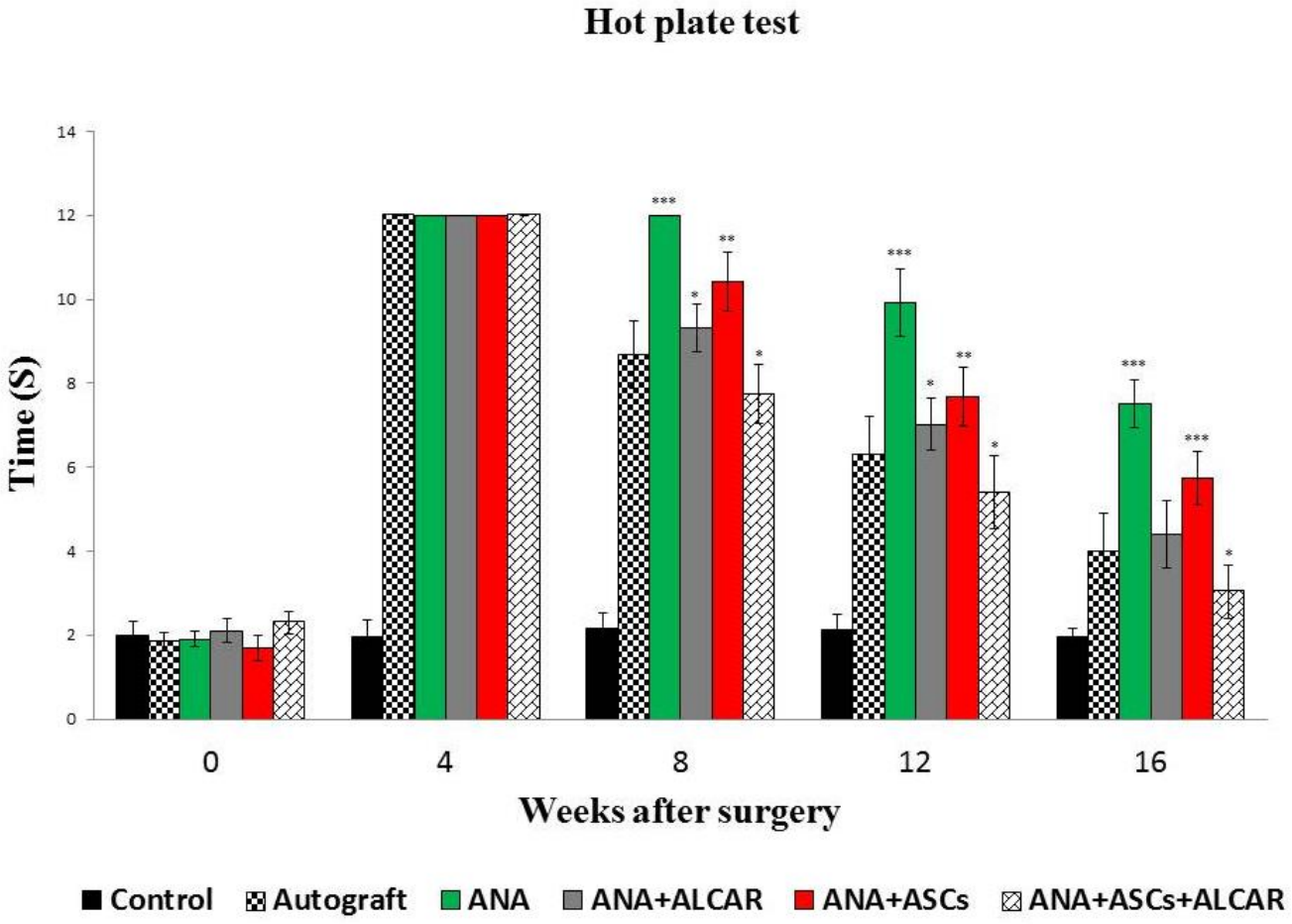

JPET Fast Forward. Published on December 27, 2018 as DOI: 10.1124/jpet.118.254540
This article has not been copyedited and formatted. The final version may differ from this version.

JPET#254540

Fig 9

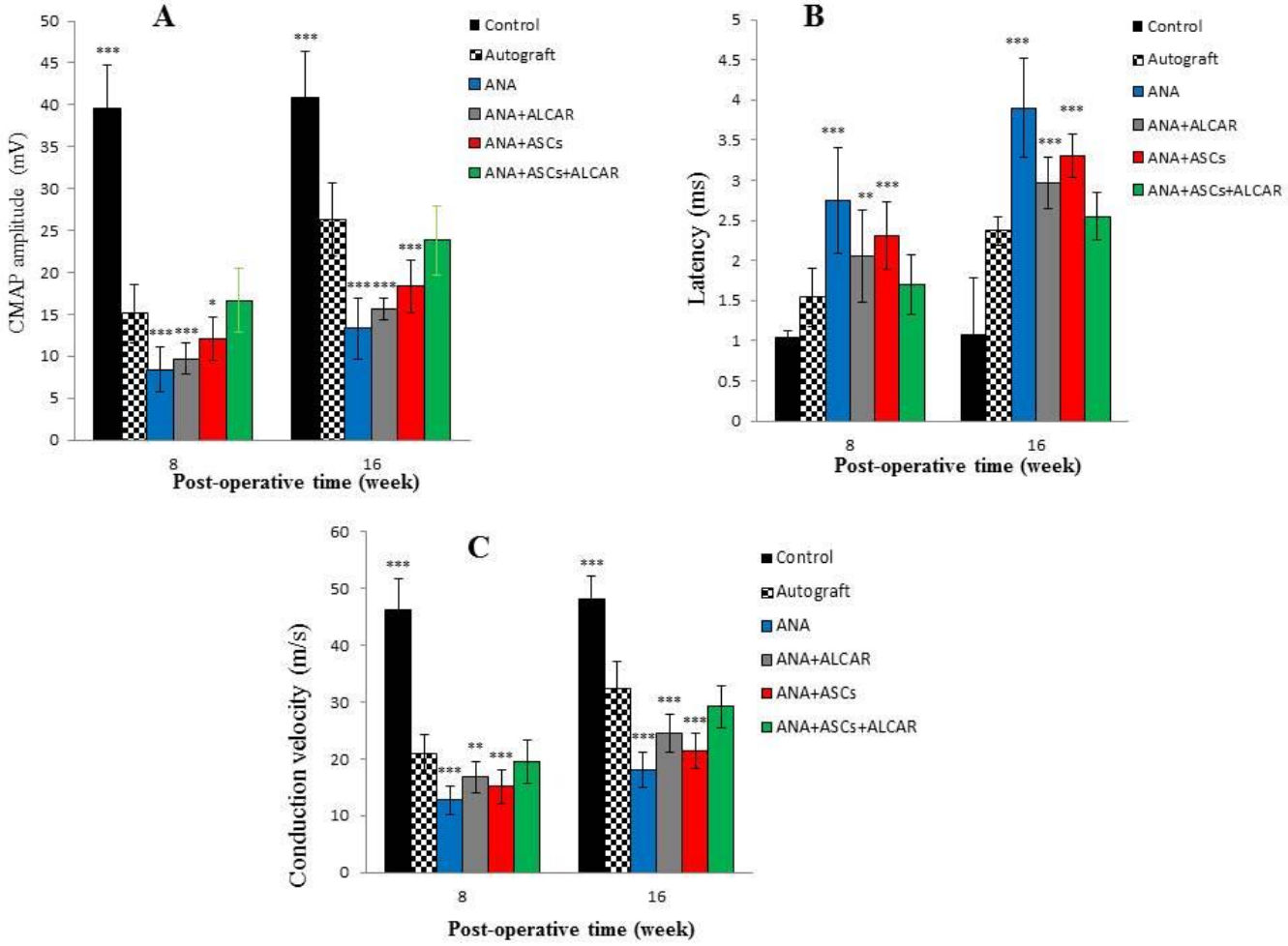

JPET Fast Forward. Published on December 27, 2018 as DOI: 10.1124/jpet.118.254540
This article has not been copyedited and formatted. The final version may differ from this version.

JPET#254540

Fig 10

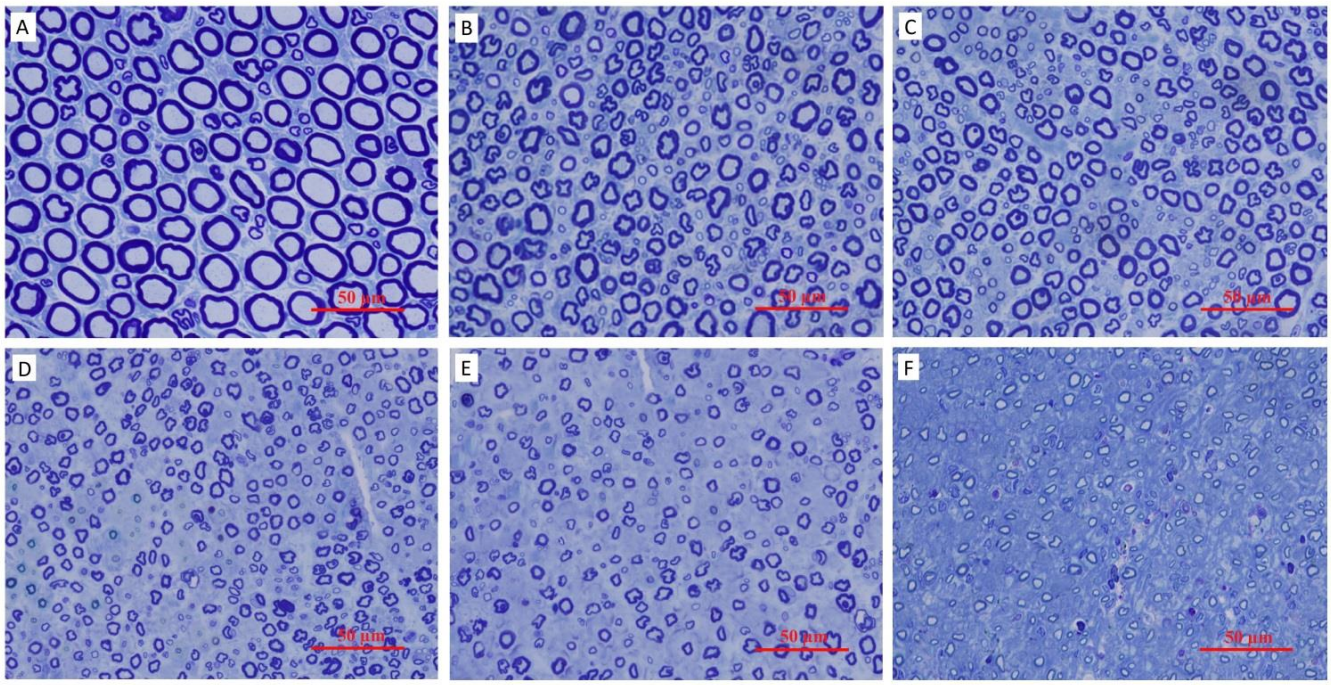

JPET Fast Forward. Published on December 27, 2018 as DOI: 10.1124/jpet.118.254540
This article has not been copyedited and formatted. The final version may differ from this version.

JPET#254540

Fig 11

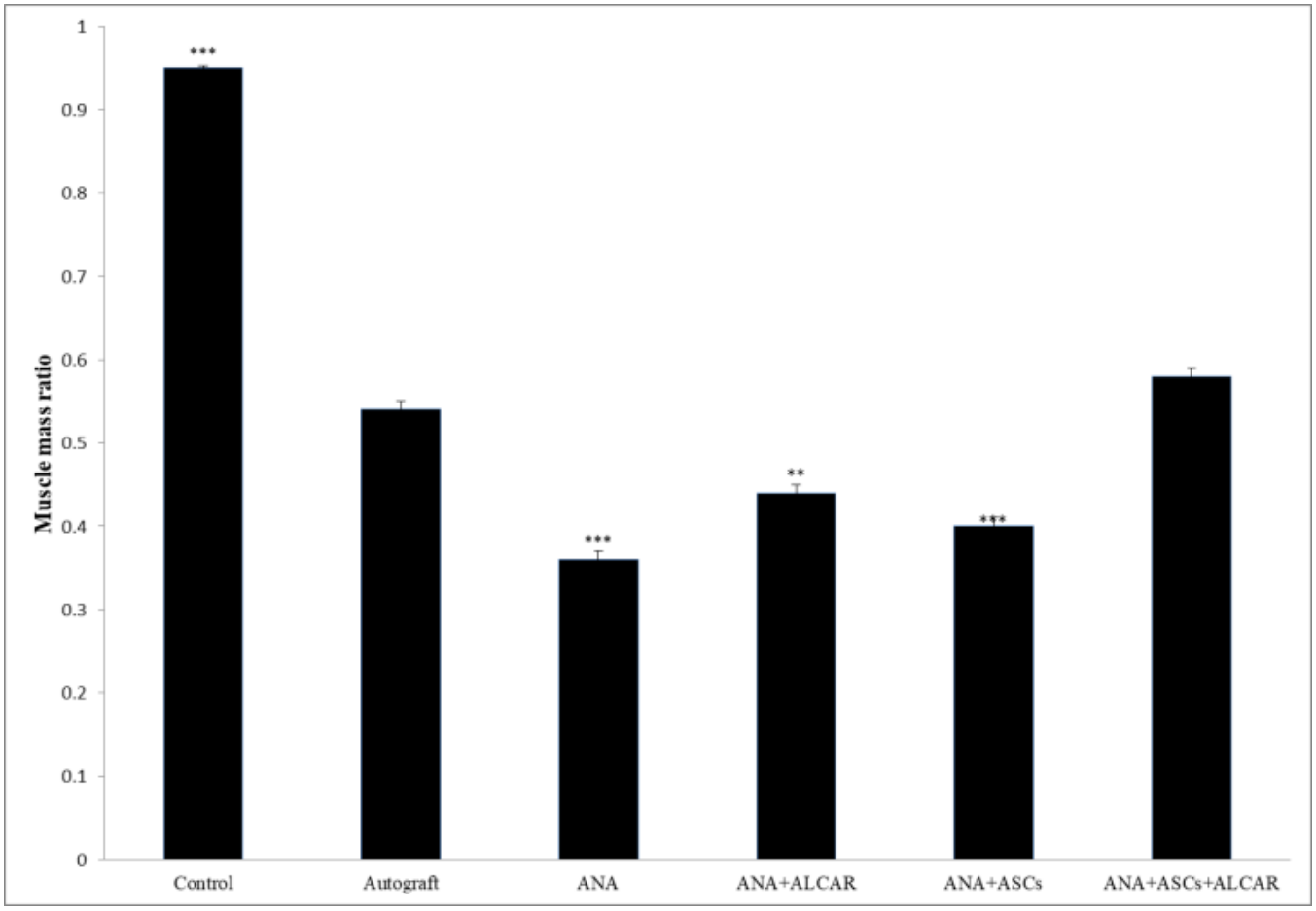

JPET Fast Forward. Published on December 27, 2018 as DOI: 10.1124/jpet.118.254540
This article has not been copyedited and formatted. The final version may differ from this version.

Fig 12